

L. ADAMCZYK*, A. PIETRUSIAK*, H. BALA*

PROTECTIVE PROPERTIES OF PEDOT/ABA COATINGS DEPOSITED FROM MICELLAR SOLUTION ON STAINLESS STEEL

WŁAŚCIWOŚCI OCHRONNE POWŁOK PEDOT/ABA OSADZANYCH Z ŚRODOWISKA MICELARNEGO NA STALI NIERDZEWNEJ

Composite coatings, consisting of combinations of the conducting polymer poly(3,4-ethylenedioxythiophene) (PEDOT) and 4-aminobenzoic acid (ABA), were electrodeposited on glassy carbon and X20Cr13 stainless steel by cyclic voltammetry, using a sodium dodecylsulfate (SDS) micellar aqueous solution of EDOT and ABA as a reaction medium. The coating deposition potential range, scan rate and composition of modification solution were determined. The protective properties of the resulting films on stainless steel were investigated in acidified (pH=4) 0.25 M sulphate solution in the absence and in presence of 0.5 M chloride ions. Diagnostic experiments include measurements of open circuit potential versus exposure time and potentiodynamic polarisation tests. Morphology of the obtained composite coatings was examined using optical metallographic microscope.

The composite coatings provide good adherence to the steel substrate and very effective steel corrosion protection. The PEDOT/ABA coatings allow to stabilize the steel corrosion potential within the passive region both in absence and in presence of chloride ions.

Keywords: Conducting polymers, poly(3,4-ethylenedioxythiophene, 4-aminobenzoic acid, micellar modification solution, anticorrosion coating, stainless steel

Powłoki kompozytowe, na bazie polimeru przewodzącego- poli(3,4-etylenodioksytiofenu) (PEDOT) i kwasu 4-aminobenzoowego (ABA), osadzano na powierzchni węgla szklistego i stali nierdzewnej X20Cr13 przy użyciu metody woltamperometrii cyklicznej. Do osadzania powłok zastosowano wodne roztwory dodecylosiarczanu sodu (SDS) zawierające EDOT i ABA. Zbadano wpływ zakresu potencjału osadzania, szybkości przemiatań potencjałem i składu roztworu modyfikacyjnego na efektywność procesu elektroosadzania powłok. Właściwości ochronne powłok uzyskanych na stali nierdzewnej badano w kwaszonych (pH=4) roztworach 0,25 M siarczanowych niezawierających i zawierających dodatek 0,5 M jonów chlorkowych. Zbadano zależność potencjału stacjonarnego od czasu wytrzymania w roztworze korozyjnym oraz wykonano potencjodynamiczne krzywe polaryzacji. Morfologię powłok zbadano przy pomocy metalograficznego mikroskopu optycznego.

Uzyskane powłoki wykazują dobrą adhezję do podłoża stali i efektywnie zabezpieczają stal przed korozją. Powłoki PEDOT/ABA stabilizują potencjał korozyjny chronionej stali zarówno w środowisku niezawierającym jak i zawierającym jony chlorkowe.

1. Introduction

In recent years, a considerable attention has been paid to conductive polymers owing to their unique combination of favourable properties like chemical stability, electrical conductivity, good catalytic properties, optical and magnetic properties. [1-5]. For these reasons, conducting polymers have been considered for many applications including development of charge storage devices and batteries [6, 7], matrices for catalysts [8, 9] or redox capacitors [10, 11]. Another area where conducting polymers could find great potential applications

is corrosion protection. Following DeBerry's work [12] on the corrosion-protective properties of polyaniline on stainless steel, many papers have been published describing corrosion studies of conducting polymers on various active metals. Protective coatings from conductive polymers were deposited on Al [13], Fe [14], Zn [15], Mg [16], Ti [17], Ni [18] and on steels [4, 19, 20]. Conducting polymers films deposited on metals have been demonstrated to stabilize a stationary potential within passive range which protects metal against its active dissolution [21, 22]. Most of efforts reported to date have involved polyaniline [19, 21], polypyrrole [4, 20] and

* CZESTOCHOWA UNIVERSITY OF TECHNOLOGY, DIVISION OF CHEMISTRY, DEPARTMENT OF MATERIALS PROCESSING, TECHNOLOGY AND APPLIED PHYSICS, 42-200 CZESTOCHOWA, 19 ARMII KRAJOWEJ AL., POLAND

polythiophene [23] (or their derivatives) for metal corrosion protection.

Poly(3,4-ethylenedioxythiophene) (PEDOT) is conductive polymer of polythiophene (PTh) class, which exhibits high stability, good conductivity and electrochromic properties [24-31]. As compared to the thiophene (Th), the 3,4-ethylenedioxythiophene (EDOT) has lower oxidation potential, what is important in anti-corrosion applications. Corrosion protection using PEDOT was first reported by Sakmeche et al. [23]. Since then, there is only few paper works about this problem [32-34]. The limitation in application of anticorrosion PEDOT coatings is their poor adherence to the metal substrate and low solubility of the monomer (EDOT) in aqueous solution (this is why most of work concerns to organic solvents [35, 36]).

In our previous works [37, 38] it was proposed to use the composite coatings based on 3,4-ethylene-dioxythiophene (EDOT) and 4-aminobenzoic acid (ABA) for protection of stainless steel against corrosion. The PEDOT/ABA coatings were deposited from 0.1 mol dm^{-3} H_2SO_4 aqueous solution using the cyclic voltammetry method. The study showed that application of ABA in the composition of the conductive polymer distinctly improved the coating adhesion to the steel. Unfortunately, the poor solubility of the monomer in aqueous solution worsens the efficiency of the process. According to literature reports [23, 39], electropolymerization of thiophene and its derivatives can be effectively carried out in aqueous solutions containing surfactants. Sakmeche et al. [23], proposed the use of an aqueous anionic micellar medium containing sodium dodecylsulfate (SDS) for PEDOT electropolymerization. Presence of the surfactant in modification solution is prone to a decrease of EDOT oxidation potential on platinum substrate as compared with the approach with a use of organic solvents [40]. In aqueous micellar solution the effective concentration of monomer is higher and the number of active sites of polymerization increases [23, 40- 42].

The present work describes the electrodeposition process and the quality of PEDOT/ABA films formed from aqueous micellar solution with sodium dodecylsulfate (SDS) as surfactant. The coatings were obtained by cyclic voltammetry method on X20Cr13 stainless steel and on glassy carbon electrode (GCE). The experimental conditions (such as potential range, scan rate and modification solution composition) were optimized in the present study. The protective properties of PEDOT/ABA coatings were evaluated in acidified (pH=4) sulphate solution without- and with addition of chloride ions.

2. Experimental

Analytically pure 4-aminobenzoic acid (ABA) and 3,4-ethylenedioxythiophene were purchased from Sigma. Sodium dodecylsulfate salt was obtained from Aldrich. Other reagents were also of analytical reagent grade and used as received. The solutions were prepared from the distilled and subsequently deionized water. The solutions are being freshly prepared for each surface modification.

Samples of commercially available stainless steel (X20Cr13) containing (in wt %) C (0.17), Cr (12.6), Si (0.34), Ni (0.25), Mn (0.30), V (0.04), P (0.024) and S (<0.005) were used in the form of disks (operating surface area, 0.2 cm^2) as electrode substrates. Prior to each experiment, the electrode surfaces were polished with waterproof emery paper (No. 600, 1000 and 2000) and rinsed with distilled water. In order to characterize basic electrochemical properties of PEDOT/ABA films, glassy carbon (from CH Instruments 104, USA) was used as an inert electrode substrate (geometric working area, 0.13 cm^2). Glassy carbon electrode was activated by polishing with aqueous alumina slurries (grain size, $0.05 \mu\text{m}$) on a polishing cloth and rinsed with distilled water.

All electrochemical experiments were carried out using CH Instruments 660 electrochemical station (Austin, USA) at a temperature of $20 \pm 2^\circ\text{C}$. A three-electrode electrochemical cell was used with a glassy carbon or stainless steel as working electrodes, a spiral platinum wire as counter electrode and a saturated calomel electrode (SCE) as reference electrode.

The electrochemical modification on X20Cr stainless steel substrate was performed in aqueous micellar solution containing: 0.1 mol dm^{-3} EDOT + 0.01 mol dm^{-3} ABA + 0.14 mol dm^{-3} SDS + 0.1 mol dm^{-3} H_2SO_4 . PEDOT/ABA films were obtained by cyclic voltammetry with potential scanning rate of 50 mVs^{-1} from -0.2 to 1.3 V (versus Ag/AgCl). After modification, the tested electrode was eventually rinsed with deionized water, and then was ready for characterization. Voltammetric responses were recorded in 0.5 mol dm^{-3} H_2SO_4 with potential ranging from 0.0 V to 0.9 V (scan rate, 50 mVs^{-1}). Topography of the tested coatings was evaluated using a metallographic microscope from Olympus (GX51). The adhesion tests were carried out by ScotchTM tape after each film deposition.

To characterize the corrosion behavior of uncovered and covered samples, the potentiodynamic polarization curves were recorded at 10 mV s^{-1} scan rate, by potential change between -0.8 and $+1.6 \text{ V}$ (vs SCE) in acidified 0.25 mol dm^{-3} K_2SO_4 (pH=4) solutions without and with addition of 0.5 mol dm^{-3} KCl.

3. Results and discussion

To determine the most effective conditions for electrochemical deposition of PEDOT/ABA coatings a series of measurements were carried out. The potential range, scan rate and composition of the solution (concentrations of ABA and monomer in modification solution) were optimized for film electrodeposition process on glassy carbon electrode (GCE). Then, the electrodeposition parameters (with steady-state conditions) and the quality of PEDOT/ABA films formed on X20Cr13 stainless steel were reported.

3.1. Electrochemical deposition of PEDOT/ABA coatings on glassy carbon substrate

In initial attempts, the optimum potential range for PEDOT/ABA films deposition from aqueous micellar solution has been determined. The potential range was selected so as to ensure both oxidation of amino group in ABA (0.8 V to 1.0 V) [43, 44] and oxidation of monomer (0.8 V to 1.2 V) [23]. A series of electrodepositions were performed by cyclic voltammetry from a start potential equal to -0.2 V to a final potential value of E_f , varying from +0.9 V to 1.3 V. Fig. 1 illustrates an example of the first cycle of the electrodeposition process of PEDOT/ABA film on GCE.

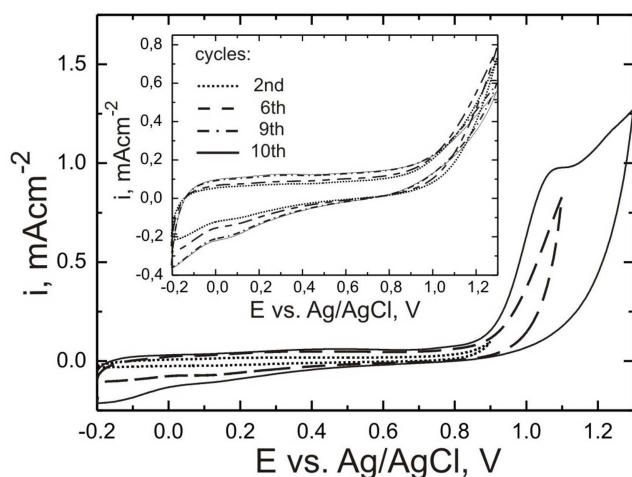


Fig. 1. Cyclic voltammograms illustrating the first cycle of PEDOT/ABA electrodeposition on the GCE substrate, $E_f = +0.9$ V (dotted line), $E_f = +1.1$ V (dashed line), $E_f = +1.3$ V (solid line). Inset: following cycles of electrodeposition for $E_f = 1.3$ V. Scan rate, 50 mVs^{-1}

As it is seen from Fig. 1, the final potential equal to 0.9 V (or 1.1 V) is not sufficient for electrodeposition of PEDOT/ABA coatings. By increasing E_f to 1.3 V, followed by oxidation of the coatings components (ABA and EDOT), the film starts growing. The oxidation begins at the first cycle and takes place when the potential becomes more noble than 1.1 V, which is confirmed by

the rise of current intensity. The following cycles (inset in Fig. 1) illustrates the successive growth of composite layers. In several first cycles, the oxidation and reduction current densities increased gradually, however, in subsequent cycles, the growth rate of the film became distinctly slowed and measured current densities stabilized.

Fig. 2 shows voltammetric responses obtained for PEDOT/ABA coatings deposited on GCE in various potential ranges (from -0.2 to 0.9 V to -0.2 to 1.3 V). In applied potential range, there were not observed any oxidation nor reduction peaks, which indicates on capacitive properties of the film [1]. Voltammetric responses for PEDOT/ABA films deposited at potential ranges -0.2 to 1.2 V and -0.2 to 1.3 V show similar plots, but a little higher oxidation- and reduction current densities were obtained for the film deposited in second potential range.

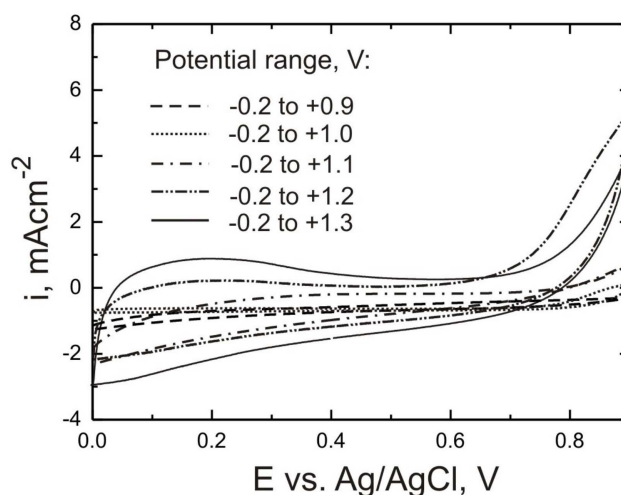


Fig. 2. Voltammetric responses recorded in $0.5 \text{ mol dm}^{-3} \text{ H}_2\text{SO}_4$ for the PEDOT/ABA films deposited in different potential range. Scan rate, 50 mVs^{-1}

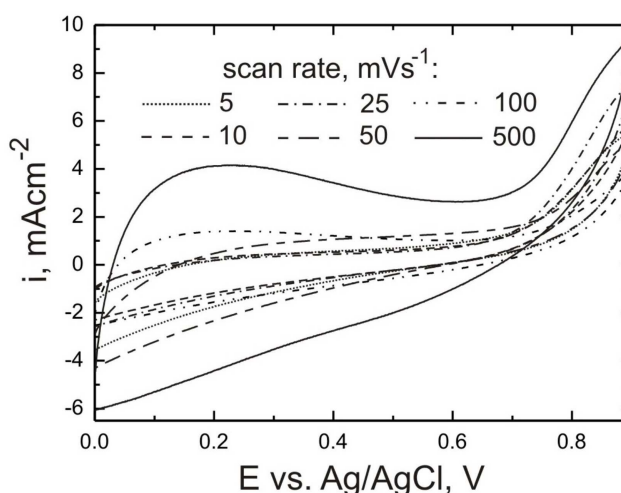


Fig. 3. Voltammetric responses recorded in $0.5 \text{ mol dm}^{-3} \text{ H}_2\text{SO}_4$ for the PEDOT/ABA films deposited on GCE at different scan rates

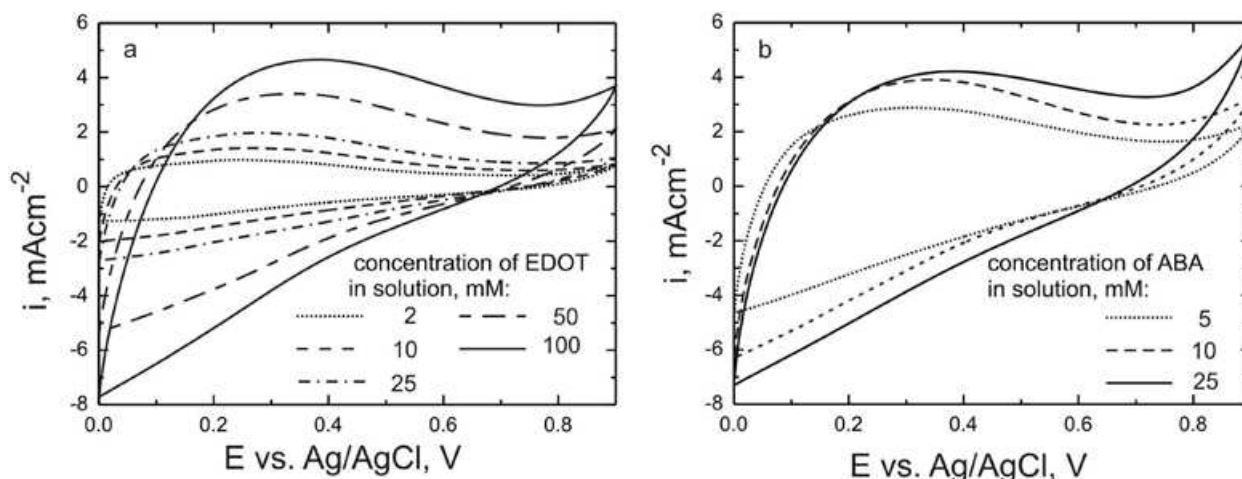


Fig. 4. Voltammetric responses recorded in $0.5 \text{ mol dm}^{-3} \text{ H}_2\text{SO}_4$ for the PEDOT/ABA films on the GCE of the solution containing different concentration of (a) EDOT and (b) ABA. Scan rate, 50 mVs^{-1}

Fig. 3 illustrates cyclic voltammetry responses obtained for PEDOT/ABA coatings on GCE at some various potential scan rates. As it is seen in Fig. 3, voltammetric response current increases with increasing scan rate of the deposition process. Voltammetric responses obtained for PEDOT/ABA coatings deposited at a scan rates ranging from 5 to 50 mVs^{-1} are similar. Greater differences in current densities are observed for coatings deposited at higher scan rates (100 , and particularly 500 mVs^{-1}). However, microscopic observations and ScotchTM tests have shown that these latest coatings exhibit worse homogeneity and rather poor adhesion. This is why we have chosen 50 mVs^{-1} as the most advantageous scan rate for electrodeposition process.

In order to put forward optimal conditions to obtain highly effective PEDOT/ABA films, we tested the effects of monomer- and 4-aminobenzoic acid concentrations in modification solution. In Fig. 4 the corresponding voltammetric responses are presented. The responses in Fig. 4a were obtained for PEDOT/ABA coatings deposited from aqueous micellar solution containing constant concentrations of ABA (0.01 M), SDS surfactant (0.14 M) and basic electrolyte ($0.1 \text{ M H}_2\text{SO}_4$), but different concentrations of EDOT. As it can be noticed from Fig. 4a, the voltammetric currents clearly increase with increase of EDOT concentration in the modification solution.

Fig. 4b shows the voltammetric responses obtained for PEDOT/ABA coatings deposited from aqueous micellar solution containing constant concentration of monomer- EDOT (0.01 M), SDS surfactant (0.14 M) and basic electrolyte ($0.1 \text{ M H}_2\text{SO}_4$), but different concentrations of ABA. All the curves from Fig. 4b are similar, and they show only small differences in the current densities. As it follows from microscopic observations and adhesion tests, the most advantageous physicochemical

properties exhibits the PEDOT/ABA coating obtained from solution containing 10 mM of ABA.

3.2. Electrochemical deposition of PEDOT/ABA coatings on X20Cr13 stainless steel

The research presented in the previous section allowed to establish the optimal conditions for electrodeposition of PEDOT/ABA coatings on X20Cr13 stainless steel substrate. Thus, the electrodeposition process on stainless steel was carried out in aqueous micellar solution containing: $0.1 \text{ M EDOT} + 0.01 \text{ M ABA} + 0.14 \text{ M SDS} + 0.1 \text{ M H}_2\text{SO}_4$. The coatings were deposited at potential range from -0.2 V to $+1.3 \text{ V}$ and at potential sweep rate 50 mVs^{-1} .

Fig. 5a illustrates comparison of first cycles of electrodeposition process of PEDOT/ABA coatings on stainless steel and glassy carbon electrodes. The irreversible oxidation peak is observed at about 1.1 V (for GCE) and 1.2 V (for stainless steel). At these potentials, the oxidation of both amino group in ABA and monomer proceed. The peak current decreases gradually with the subsequent potential scanning cycles. As we can see from insert in Fig. 5, in first cycle of deposition, oxidation of steel takes place (irreversible peak from -0.4 V to $+0.2 \text{ V}$). This peak corresponds to active dissolution of steel followed by formation of passive layer ($E > 0.2 \text{ V}$). At $E > +1.0 \text{ V}$ the anodic currents start going to grow, which can be ascribed to oxidation of film components (amine group in ABA and EDOT monomer) and beginning of film deposition. The further increase of the anodic current ($E > +1.2 \text{ V}$) is connected with transpassivation of steel (oxidation of Cr(III) oxide to CrO_4^{2-}) [45]. In Fig. 5b voltammetric responses obtained for PEDOT/ABA coatings on GCE and stainless steel are compared.

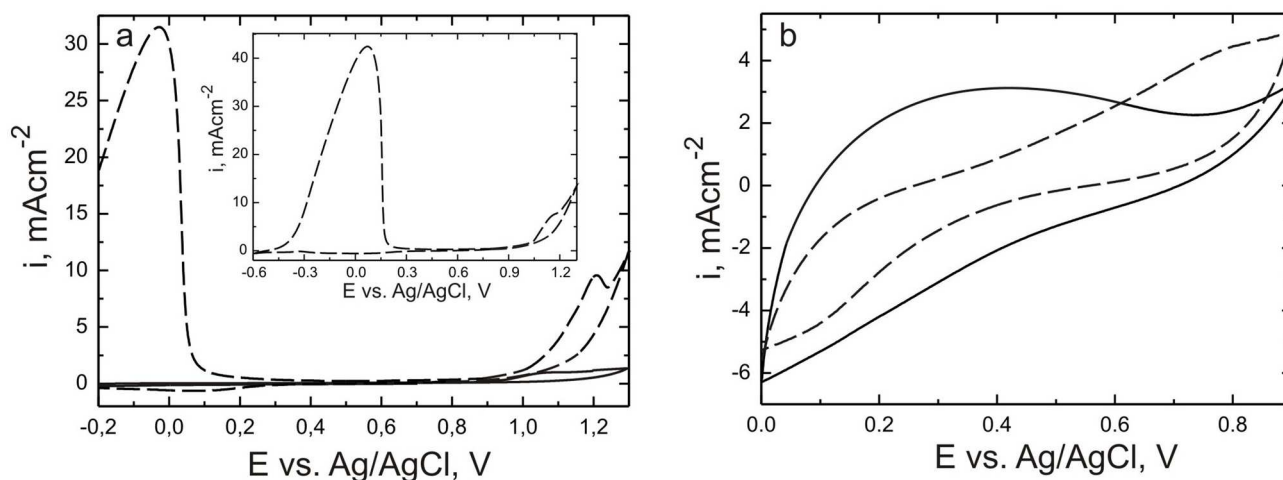


Fig. 5. (a) Cyclic voltammograms illustrating the first cycle electrodeposition of PEDOT/ABA film on GCE (solid line) and stainless steel (dashed line). Inset: First cycle deposition of the film on stainless steel measured at wide potential range. (b) Voltammetric responses recorded in $0.5 \text{ mol dm}^{-3} \text{ H}_2\text{SO}_4$ for PEDOT/ABA films on GCE (solid line) and on stainless steel (dashed line). Scan rate, 50 mVs^{-1}

In order to get insight the morphology of PEDOT/ABA film electrodeposited on stainless steel, we examined its structure by metallographic microscope. As it can be seen from Fig.6 the obtained PEDOT/ABA coating is homogeneous and compact, and shows characteristic globular clusters, typical for PEDOT films [18, 23].

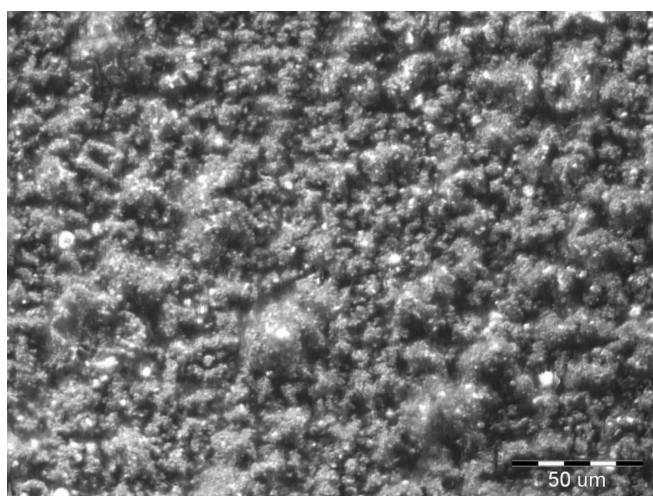


Fig. 6. The topography of the PEDOT/ABA film electrodeposited on stainless steel. Deposition time: 1000s (34 cycles)

Potentiodynamic curves for bare stainless steel and for steel covered with PEDOT/ABA film, measured in acidified sulfate solution ($\text{pH}=4$), in the absence and in the presence of 0.5 M of chloride ions, are presented in Figs. 7 and 8.

As it is seen in Fig. 7, the presence of PEDOT/ABA coatings on stainless steel has led to a significant decrease of anodic current densities especially in potential range $-0.6 \div +0.2 \text{ V}$. It is noteworthy that the corrosion potential is shifted for covered steel of about 0.3 V

towards positive values. The PEDOT/ABA coatings inhibits corrosion process in active range of about order of magnitude. The active dissolution peak of the steel (-0.4 V) is not very distinct for the applied test solution ($\text{pH}=4$) and it practically disappears for covered steel. In passive range (up to 0.9 V), the current densities for bare and covered steel are similar, however, PEDOT/ABA coating distinctly inhibits transpassive dissolution of the steel ($>1.1 \text{ V}$).

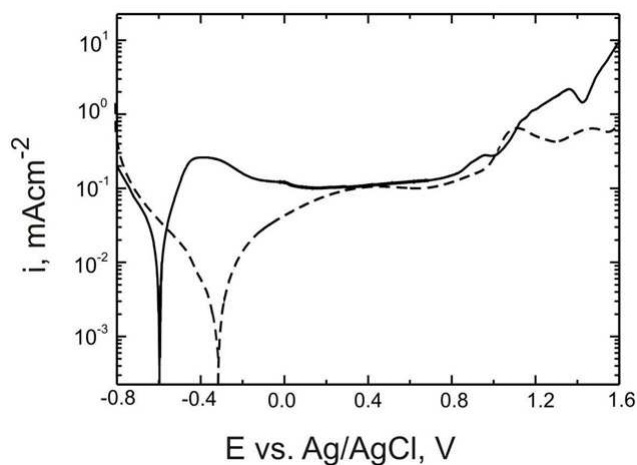


Fig. 7. Potentiodynamic curves recorded for bare stainless steel (solid line), and for stainless steel covered with PEDOT/ABA film. Electrolyte, $0.25 \text{ mol dm}^{-3} \text{ K}_2\text{SO}_4$ ($\text{pH}=4$). Scan rate, 10 mVs^{-1}

As it results from Fig. 7 and 8, in spite of the presence of chloride ions, the PEDOT/ABA coating inhibits the active dissolution of steel. What is more: in presence of PEDOT/ABA coatings steel passivates spontaneously. However, for solution containing Cl^- ions the break down of the passive layer takes place. The polarization curves indicate (Fig. 8) that the pit nucleation potential (E_{pit}) equals ca. -0.1 V for bare steel and it is signif-

icantly shifted (by about 0.3 V) towards positive value for steel covered with PEDOT/ABA coating. Moreover, for steel covered with PEDOT/ABA film the slope of anodic curve above E_{pit} is distinctly lower than that for bare steel. This is the evidence that the pits development is definitely slower for covered steel than that for bare steel.

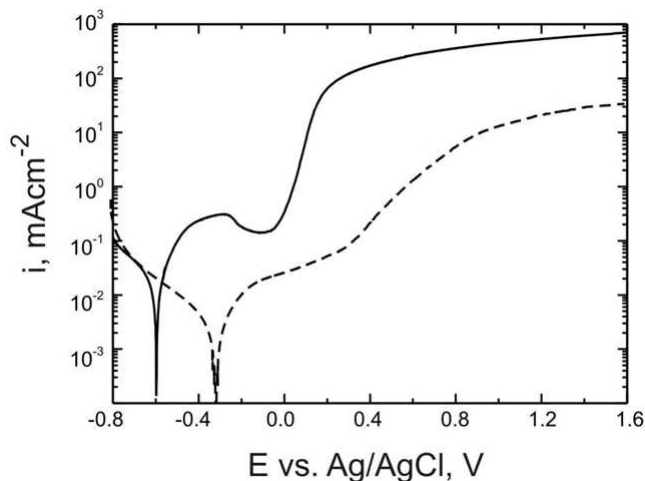


Fig. 8. Potentiodynamic curves recorded for bare stainless steel (solid line), and for stainless steel covered with PEDOT/ABA film (dashed line). Electrolyte, $0.25 \text{ mol dm}^{-3} \text{ K}_2\text{SO}_4 + 0.5 \text{ mol dm}^{-3} \text{ KCl}$ (pH=4). Scan rate, 10 mVs^{-1}

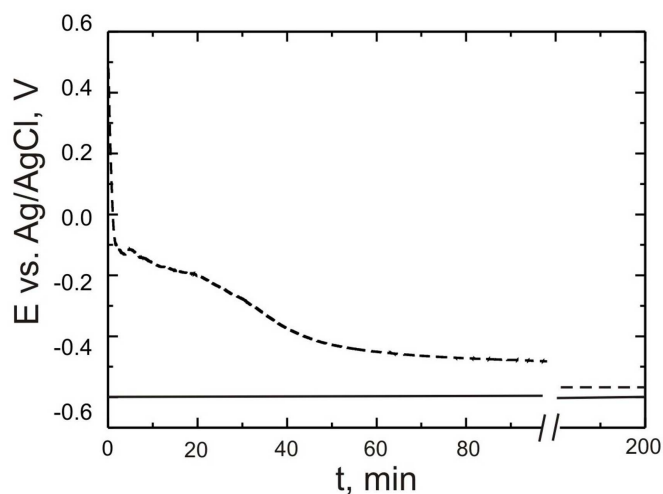


Fig. 9. Changes of open circuit potentials vs. exposure time recorded for bare stainless steel (solid line), and for stainless steel covered with PEDOT/ABA film (dashed line). Electrolyte, $0.25 \text{ mol dm}^{-3} \text{ K}_2\text{SO}_4 + 0.5 \text{ mol dm}^{-3} \text{ KCl}$ (pH=4)

In order to evaluate the kinetic stability of PEDOT/ABA films we followed through changes of the open circuit potential of stainless steel substrate uncovered and covered with PEDOT/ABA film (Fig. 9). Under such conditions, the corrosion process of bare steel proceeds at relatively fast rate, immediately after its immersion to the corrosion solution (pH=4, 0.5 M Cl^-). Modification of the steel with PEDOT/ABA coating moves

the open circuit potential (E_{corr}) in the passive range, then the corrosion potential progressively decreases versus the exposure time. The steel transition to the active range comes about 180 mins for covered steel. The plots presented in Fig. 9 testify that PEDOT/ABA coating stabilizes passive state of stainless steel in acidified solution containing 0.5 M of chloride ions for comparatively long period of time.

4. Concluding remarks

The objective of this work was the optimisation of PEDOT/ABA electrodeposition process from aqueous micellar solution. The most advantageous concentrations of EDOT (0.1 M) and ABA (0.01 M) in modification solution, ensuring effective corrosion inhibition and coating adherence to the stainless steel substrate have been determined. Obtained PEDOT/ABA surfacial films exhibit promising properties towards the protection of stainless steel against both general and pitting corrosion in acidified, chloride-containing medium.

Acknowledgements

This work was supported by Ministry of Science and Higher Education, Projects: N N507 4616 33 and N N507 5122 39

REFERENCES

- [1] G. Inzelt, *Conducting Polymers*, Springer, 2008.
- [2] G. Inzelt, M. Pineri, J.W. Schultze, M.A. Vorotyntsev, *Electrochim. Acta* **45**, 2430 (2000).
- [3] J.D. Stenger-Smith, *Prog. Polym. Sci.* **23**, 57 (1998).
- [4] C.A. Ferreira, S. Aeiayach, J.J. Aaron, P.C. Lacaze, *Electrochim. Acta* **41**, 1801 (1996).
- [5] P. Zarras, N. Anderson, C. Webber, D.J. Irvin, J.A. Irvin, A. Guenther, J.D. Stenger-Smith, *Rad. Phys. & Chem.* **68**, 387 (2003).
- [6] D.G. Shchukin, K. Kohler, H. Mohwald, *J. Am. Chem. Soc.* **128**, 4560 (2006).
- [7] Q. Zhoi, C.M. Li, J. Li, X. Cui, D. Gervasio, *J. Phys. Chem. C* **111**, 11216 (2007).
- [8] Y. C. Liu, B.J. Hwang, W.C. Hsu, *Sens. Actuators B* **87**, 304 (2002).
- [9] S. Cosnier, R.E. Ionescu, S. Herrmann, L. Bouffier, M. Demeunynck, R.S. Marks, *Anal. Chem.* **78**, 7054 (2006).
- [10] K.H. An, K.K. Jeon, J.K. Hea, S.C. Lim, D.J. Bae, Y.H. Lee, *J. Electrochem. Soc.* **149**, A1086 (2002).
- [11] M.D. Ingram, H. Staesche, K.S. Ryder, *J. Power Sources* **129**, 107 (2004).

- [12] D.W. DeBerry, J. Electrochem. Soc. **132**, 1022 (1985).
- [13] K. Naoi, M. Takeda, H. Kanno, M. Sakakura, A. Shimada, Electrochim. Acta **45**, 3413 (2000).
- [14] H. Nguyen, T. Le, B. Garcia, C. Deslouis, Q.L. Xuan, Electrochim. Acta **46**, 4259 (2001).
- [15] J. Petitjean, S. Aeiyaich, J.C. Lacroix, P.C. Lacaze, J. Electroanal. Chem. **478**, 92 (1999).
- [16] V.T. Truong, P.K. Lai, B.T. Moore, R.F. Muscat, M.S. Russo, Synth. Met. **110**, 7 (2000).
- [17] K. Idla, O. Inganas, M. Strandberg, Electrochim. Acta **45**, 2121 (2000).
- [18] F. Lallemand, F. Plumier, J. Delhalle, Z. Mekhalif, Appl. Surf. Sci. **254**, 3318 (2008).
- [19] A.A. Hermas, M. Nakayama, K. Ogura, Electrochim. Acta **50**, 2001 (2005).
- [20] O. Iroh, W. Su, Electrochim. Acta **46**, 15 (2000).
- [21] W.K. Lu, R.L. Elsenbaumer, B. Wessling, Synth. Met. **71**, 2163 (1995).
- [22] M.K. Rokovic, K. Kvastek, V. Horvat-Radošević, L. Duic, Corr. Sci. **49**, 2567 (2007).
- [23] N. Sakmeche, J.J. Aaron, S. Aeiyaich, P.C. Lacaze, Electrochim. Acta **45**, 1921 (2000).
- [24] X. Du, Z. Wang, Electrochim. Acta **48**, 1713 (2003).
- [25] A. Moliton, R.C. Hiorns, Polym. Internat. **53**, 1397 (2004).
- [26] L. Groenendaal, F. Jonas, D. Freitag, A. Pielartzik, J.R. Reynolds, Adv. Mater. **12**, 481 (2000).
- [27] F. Jonas, J.T. Morrison, Synth. Metal **85**, 1397 (1997).
- [28] G. Heywang, F. Jonas, Adv. Mater. **4**, 116 (1992).
- [29] H.W. Heuer, R. Wehrmann, S. Kirchmeyer, Adv. Funct. Mater. **12**, 89 (2002).
- [30] T.Y. Kim, J.E. Kim, Y.S. Kim, T.H. Lee, W.J. Kim, K.S. Suh, Curr. Appl. Phys. **9**, 120 (2009).
- [31] A. Zykwińska, W. Domagała, B. Pilawa, M. Lapkowski, Electrochim. Acta **50**, 1625 (2005).
- [32] L. Adamczyk, P.J. Kulesza, H. Bala, Physicochem. Mech. Mater. **7**, 368 (2008).
- [33] D. Aradilla, C. Ocampo, E. Armelin, C. Aleman, R. Oliver, F. Estrany, Mater. & Corr. **58**, 867 (2007).
- [34] E. Armelin, A. Meneguzzi, C.A. Ferreira, C. Aleman, Surf. Coat. Tech. **203**, 3763 (2009).
- [35] J.Y. Kim, J.H. Jung, D.E. Lee, J. Joo, Synth. Met. **126**, 311 (2002).
- [36] T.Y. Kim, C.M. Park, J.E. Kim, K.S. Suh, Synth. Met. **149**, 169 (2005).
- [37] L. Adamczyk, A. Pietrusiak, Ochr. przed Korozją, Nr 11, 465 (2009).
- [38] A. Pietrusiak, L. Adamczyk, Ochr. przed Korozją, Nr 4-5, 302 (2010).
- [39] A. Petr, F. Zhang, H. Peisert, M. Knupfer, L. Dunsch, Chem. Phys. Letters **385**, 140 (2004).
- [40] N. Sakmeche, E.A. Bazzaooui, M. Fall, S. Aeiyaich, M. Jouini, J.C. Lacroix, J.J. Aaron, P.C. Lacaze, Synth. Met. **84**, 191 (1999).
- [41] N. Sakmeche, J.J. Aaron, M. Fall, S. Aeiyaich, M. Jouini, J.C. Lacroix, P.C. Lacaze, Langmuir **15**, 2566 (1999).
- [42] N. Sakmeche, J.J. Aaron, M. Fall, S. Aeiyaich, M. Jouini, J.C. Lacroix, P.C. Lacaze, J. Chem. Soc. Chem. Commun. 2727 (1996).
- [43] G. Yang, Y. Shen, M. Wang, H. Chen, B. Liu, S. Dong, Talanta **68**, 741 (2006).
- [44] A. Pietrusiak, L. Adamczyk, H. Bala, Ochr. przed Korozją, Nr 4-5, 188 (2009).
- [45] K. Jagielska-Wiaderek, H. Bala, P. Wieczorek, J. Rudnicki, D. Kumecka-Tatar, Arch. Metall. Mater. **54**, 115 (2009).